RSC Advances

PAPER

View Article Online
View Journal | View Issue

Cite this: *RSC Adv.*, 2020, **10**, 4310

Understanding the correlation between structure and dynamics of clocortolone pivalate by solid state NMR measurement

Krishna Kishor Dey, [a] Shovanlal Gayen[b] and Manasi Ghosh *[a]

Structural characteristics of clocortolone pivalate are unique in the topical corticosteroid field having high penetration power through the stratum corneum of skin as well as low corticosteroid-related adverse effects. The molecule was thoroughly studied by ^{13}C 2DPASS CP MAS NMR and spin–lattice relaxation time measurements. Molecular correlation time at different carbon nuclei positions was calculated by assuming that the chemical shift anisotropy interaction and heteronuclear dipole–dipole interaction play vital roles in the ^{13}C spin–lattice relaxation mechanism. The CSA parameters are substantially varied at different carbon nuclei sites. This suggests that the electronic distribution surrounding the carbon nuclei varies widely when the same carbon atom is placed in different chemical surroundings of the molecule. The spinning CSA sideband pattern for C11, C17, C26 nuclei is axially symmetric. The asymmetry parameter is very small ($\leq$0.3) for C2, C5, C10, C22, C23, C24 nuclei, and it is reasonably high ($\geq$0.9) for C3, C4, C6, C18, C19, C21 nuclei. The anisotropy parameter is very high for double bonded C14, C15, C18, C19, C21, C22, and C23 nuclei. Spin–lattice relaxation time and molecular correlation time are also varied substantially for carbon nuclei situated at various positions of the molecule. The spin–lattice relaxation time is slow for carbon nuclei residing at the carbon ring, and it is very fast for C12, C17, C16, C26 carbon nuclei situated at the side portion of the molecule. Molecular correlation time is of the order of 10^{-4} s for those carbon nuclei attached with neighbouring carbon or oxygen atoms by double bonds like C14, C15, C18, C19, C21, C22, and C23. It implies that the molecular correlation time is very high for those carbon nuclei associated with high values of the chemical shift anisotropy parameter. In contrast, the molecular correlation time is of the order of 10^{-8} s for C12, C16, and C17 carbon nuclei. From these studies, it is clear that the various portions of the molecule exhibit different degrees of motion and the dynamics is related with the structural characteristics of the molecule. These investigations on important drug clocortolone pivalate by solid state NMR will help researchers to understand the structure and dynamics of the molecule, which will give a direction to develop advance corticosteroids.

Received 25th November 2019
Accepted 9th January 2020

DOI: 10.1039/c9ra09866f

rsc.li/rsc-advances

1. Introduction

Introduction of topical glucocorticoids has led marked improvement in the outcomes of several skin diseases. For many years, they have played major roles in the treatment of different dermatoses sensitive to corticosteroids. Skin diseases like atopic dermatitis, contact dermatitis, psoriasis vulgaris, seborrheic dermatitis, *etc.*, can be treated.[1–6] They are also used for the treatment of different eczematous skin disorders from different age groups of the human population, including children.[7,8] Topical corticosteroids are classified based on various potency values from class 1, most potent to least potent, class 7 based on their different skin permeation abilities, activity at the target and rate of removal from the site of application. The selection of a specific class of topical corticosteroid is influenced by its sensitivity to the disease and its penetration power to reach the site of the disease. The high potency or super high potency corticosteroids are mainly used for the treatment of Chronic Plaque Psoriasis (CPP) and lichenified eczematous plaques.[9,10] The mid potency (class 4 to 5) topical corticosteroids are applied for the treatment of various common dermatological disorders. Clocortolone pivalate is one of the widely used mid-potency (class 4) topical corticosteroid used in the treatment of different skin diseases. The use of corticosteroids in skin diseases is determined by their distinctive biological properties like anti-inflammatory, anti-miotic, immunosuppressive action and their ability to inhibit the production of connective tissue molecules.[11–24] Although topical corticosteroids lack antipruritic activity, they can function by reducing the inflammation of skin disorders and thus, they decrease indirectly the itching of different skin disorders.

[a]*Department of Physics, Dr Harisingh Gour Central University, Sagar, MP-470003, India. E-mail: manasi.ghosh@gmail.com*

[b]*Department of Pharmaceutical Sciences, Dr Harisingh Gour Central University, Sagar, MP-470003, India*

In general, the basic structure of topical corticosteroid molecules consists of 21-carbon atoms and an additional 2-carbon side chain at C5. There are three 6-carbon rings and one 5-carbon ring in its core structure. The basic structure of corticosteroid is frequently modified to enhance the glucocorticoid receptor binding affinity, lipophilicity and ability of cutaneous penetration.[8] Clocortolone pivalate is a nice example where different structural modifications have improved its properties.[13,14] Clocortolone pivalate is 4-chloro-13α-fluoro-11β, 21-dihydroxy-16α methylpregna-1,4-diene-3, 20-dione 21-pivalate. In the molecule, esterification was introduced at C20 position with a pivalate group to increase lipophilicity and decrease metabolic breakdown. Methylation at the C8 position is done to decrease various allergic reactions of corticosteroids.[10] Moreover, halogenation by fluorine and chlorine at C13 and C4 position respectively, increases the efficacy and safety profile of this mid potency topical corticosteroid.[15] Due to its unique structure having high efficacy and low side effects it is widely used as a 0.1% cream for the treatment of many skin diseases. Several clinical trials have been performed on clocortolone pivalate 0.1% cream to prove its efficacy and safety and it is eminently suitable for human use with a relative lack of adverse effects.[13–16] One of these trials includes 559 adult and paediatric volunteers, who have undergone active treatment of clocortolone pivalate cream. Overall no systemic adverse effects were reported from the study. Hence, it can be concluded that clocortolone pivalate is highly bio-available for local activity in the skin after its topical application.[17–24]

Chemical shift anisotropy (CSA) is a sensitive probe of detecting the local electronic environment, three-dimensional structural details surrounding the nucleus, and the degree of motion of the molecule. The broadening of spectral line-width due to the presence of various anisotropic interactions makes it complicated to determine the values of CSA parameters from static solid state NMR spectra. In magic angle spinning (MAS) experiment all the information encoded in anisotropic interactions are lost. However, the principal values of CSA tensor can be reconstructed by - two-dimensional MAS/CSA NMR experiment;[26] SUPER (separation of undistorted powder patterns by effortless recouplin) MAS NMR;[27] ROCSA (recoupling of chemical shift anisotropy) pulse sequence at MAS frequencies 11 to 20 kHz;[28] RNCSA (γ-encoded RN_n^ν-symmetry based chemical shift anisotropy) schemes for the system associated with weak homonuclear dipole–dipole interactions;[29] 2DMAF (two-dimensional magic angle flipping) experiment;[30–32] 2DMAT (two-dimensional magic angle turning) experiment;[33] 2DPASS (two-dimensional phase adjusted spinning side-band) MAS (magic angle spinning) SSNMR experiment.[34–36] The CSA parameters of glass compounds,[36] biopolymers,[37–40] antifungal drug itraconazole[41] were extracted by applying 2DPASS MAS NMR experiments. The purpose of the current work is to elucidate the structural details and spin dynamics of clocortolone pivalate by extracting principal values of CSA parameters by two-dimensional phase-adjusted spinning side-band (2DPASS) magic-angle-spinning (MAS) nuclear magnetic resonance (NMR) experiment, to determine the site-specific spin–lattice relaxation time by Torchia CP method,[25] and to calculate of molecular correlation time at chemically distinct carbon sites by assuming that the chemical shift anisotropy interaction and heteronuclear dipole–dipole coupling play predominate role in spin–lattice relaxation mechanism. This type of spectroscopic studies is necessary for confounding structure–dynamic relationships of steroids, which has enormous applications in pharmaceutical industry.

2. Experiment section

2.1 NMR-measurements

An active ingredient of clocortolone pivalate from Sigma Aldrich was used for solid state NMR experiments. All solid state NMR experiments were carried out on a JEOL ECX 500 NMR Spectrometer associated with a 3.2 mm JEOL double resonance MAS probe, operating at a resonance frequencies of 500 MHz for ^{1}H and 125.721 MHz for ^{13}C. The magic angle spinning (MAS) speed was 10 kHz for ^{13}C CP-MAS and Torchia CP experiments. The cross-polarization (CP) condition was maintained at contact time 2 ms, and SPINAL-64 ^{1}H decoupling. ^{13}C-spin lattice relaxation experiment was performed by following Torchia CP method.[25]

2.2 CSA measurements

2DPASS MAS SSNMR experiment generates a isotropic spectrum in direct-dimension and an anisotropic spectrum in indirect dimension. It can correlate the isotropic dimension with anisotropic dimension.[36–41,50–52] As the parameters of second rank CSA tensor corresponding to two distinct chemical environments are different, hence, with the help of this experiment, one can also identify two overlapping signals.[52] Herzfeld and Berger[42] had shown that the sideband intensities of spinning CSA sideband pattern of different nuclei are related with the CSA parameters and they had introduced a graphical method for evaluating the CSA eigenvalues.

In 1995, Antzutkin *et al.*[35] had established the pulse scheme of 2DPASS MAS NMR experiment using sequence of five π pulses. The total time duration of all the PASS sequences containing five π pulses is independent of the sideband phase shift. The time evolution of five π pulses is varied during the 2D PASS experiment according to the PASS equations. The 2DPASS experiments were carried out at two different values of MAS frequencies 600 Hz and 2000 Hz.

3. Results and discussion

3.1 Spin–lattice relaxation measurements

Fig. 1(a) shows the structure of clocortolone pivalate is associated with three 6-carbon rings and one 5-carbon ring. Fig. 1(b) represents ^{13}C-CP-MAS-NMR spectrum of clocortolone pivalate. Fig. 2 shows ^{13}C spin–lattice relaxation decay curves of clocortolone pivalate at (a) C1, (b) C9, (c) C13, and (d) C27 carbon nuclei positions. Table 1 shows the spin–lattice relaxation time of numerous carbon nuclei is varying substantially. For C5 it is 184 s and for C12, C17, C16, C26 carbon nuclei it values reduces to 1 s. At the position of C20, where the esterification was

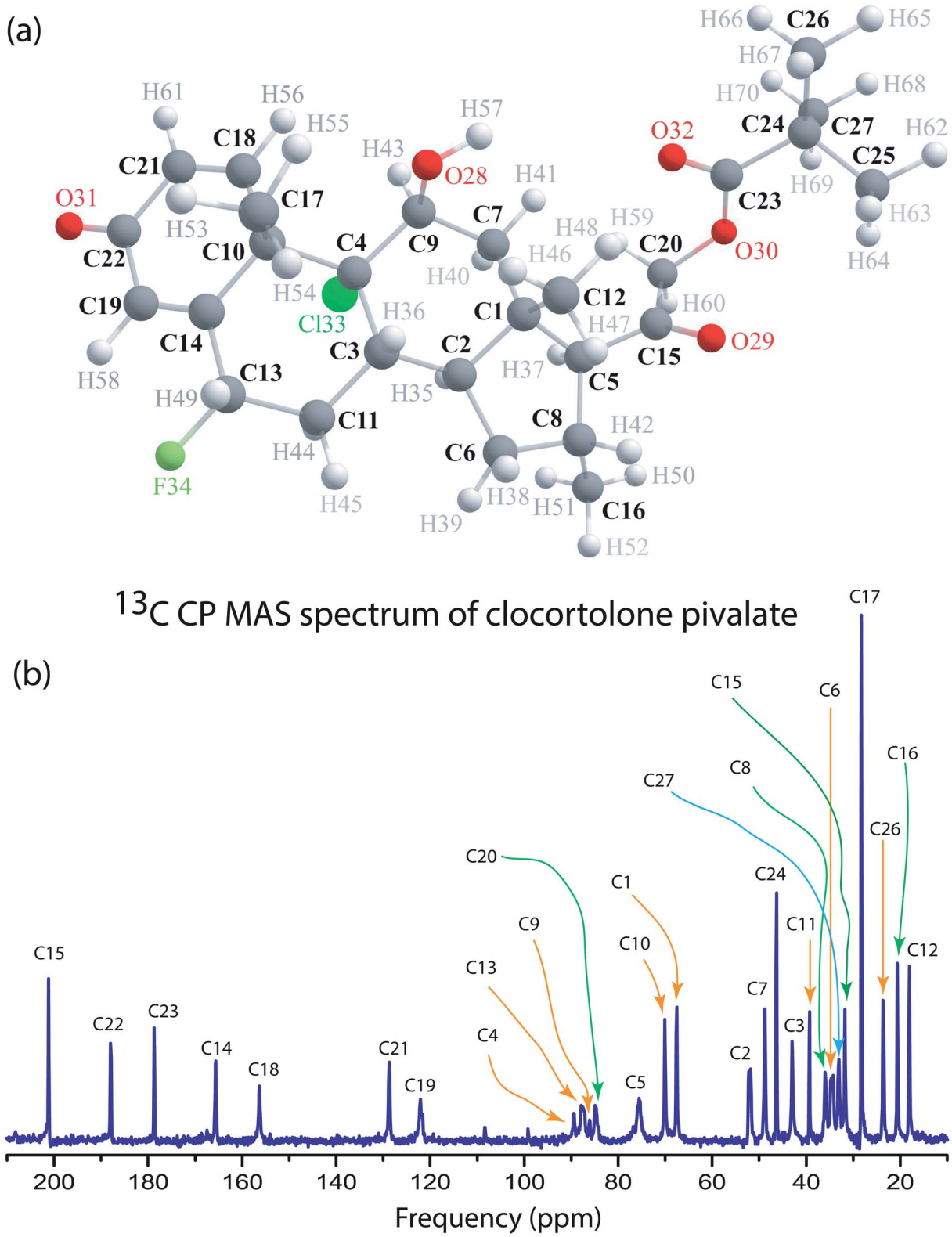

Fig. 1 (a) Molecular structure of clocortolone pivalate. (b) ^{13}C CP MAS NMR spectrum of clocortolone pivalate.

incorporated with the molecule by introducing a pivalate group for increasing lipophilicity and decreasing metabolic breakdown, the spin–lattice relaxation time is 175 s. At C8 position, where methylation is introduced to decrease various allergic reactions of corticosteroids, the value of spin–lattice relaxation is 138 s. At the positions of C4 and C13 halogenations was done by chlorine and fluorine atoms to increase the efficacy and safety profile of the drug. The spin–lattice relaxation time of C4

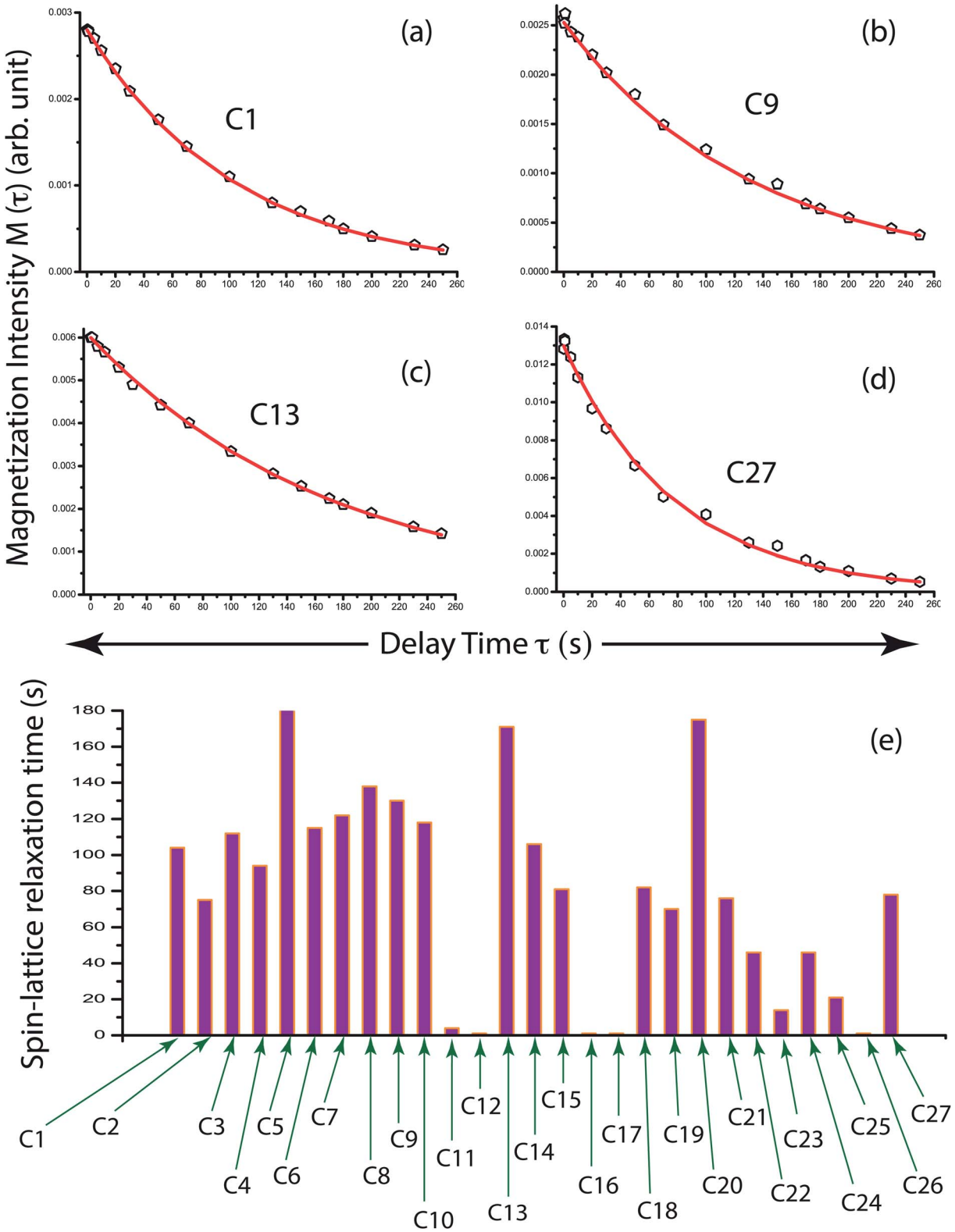

Fig. 2 ^{13}C spin–lattice relaxation decay curve of (a) C1, (b) C9, (c) C13, (d) C27. (e) shows the spin–lattice relaxation time is different at chemically distinct carbon sites of clocortolone pivalate.

and C13 are respectively 94 s and 171 s. Spin–lattice relaxation time is considerable high for those carbon nuclei reside at the carbon rings (there are three 6-carbon rings and one 5-carbon ring in the molecule) and it is comparatively lower for carbon nuclei attached at the side of the molecule like C12, C17, C16, C26 (as shown in Fig. 1(a)). The dipole–dipole interaction of those carbon nuclei resides at the side of the molecule is highly influenced by the internal motion and rotational motion of

Table 1 Spin–lattice relaxation time of clocortolone pivalate at chemically different carbon sites

^{13}C-Spin–lattice relaxation time (T_1) of clocortolone pivalate			
Carbon nuclei	Spin lattice relaxation time (T_1) (s)	Carbon nuclei	Spin lattice relaxation time (T_1) (s)
C1	104 ± 5	C2	75 ± 5
C3	112 ± 5	C4	94 ± 5
C5	184 ± 10	C6	115 ± 5
C7	122 ± 5	C8	138 ± 5
C9	130 ± 5	C10	118 ± 5
C11	4 ± 1	C12	1 ± 0.5
C13	171 ± 10	C14	106 ± 5
C15	81 ± 5	C16	1 ± 0.5
C17	1 ± 0.5	C18	82 ± 5
C19	70 ± 5	C20	175 ± 10
C21	76 ± 5	C22	46 ± 2
C23	14 ± 2	C24	46 ± 2
C25	21 ± 2	C26	1 ± 0.5
C27	78 ± 5		

molecule about its symmetry axis. That's why the degree of motion is higher for those carbon nuclei.

3.2 Chemical shift anisotropy

Chemical-shift anisotropy interaction has a great role in nuclear spin relaxation mechanism. Hence, the accurate determination of CSA tensor can provide a plenty of information about molecular structure, molecular conformation and spin dynamics. In principal axis system (PAS) off-diagonal components of CSA tensor are cancel out and three diagonal terms survive. The expression of those diagonal components of chemical shift anisotropy tensor (δ_{11}, δ_{22} and δ_{33}) are given by[43,44]

$$\delta_{33} = \frac{e^2}{2m}\left\langle 0\left|\frac{x^2+y^2}{r^3}\right|0\right\rangle - \left(\frac{e\hbar}{2m}\right)^2 \times \sum_n \left\{ \frac{\left\langle 0|L_z|n\right\rangle\left\langle n\left|\frac{2L_z}{r^3}\right|0\right\rangle}{(E_n-E_0)} + \frac{\left\langle 0\left|\frac{2L_z}{r^3}\right|n\right\rangle\left\langle n|L_z|0\right\rangle}{(E_n-E_0)} \right\} \quad (1)$$

$$\delta_{11} = \frac{e^2}{2m}\left\langle 0\left|\frac{y^2+z^2}{r^3}\right|0\right\rangle - \left(\frac{e\hbar}{2m}\right)^2 \times \sum_n \left\{ \frac{\left\langle 0|L_x|n\right\rangle\left\langle n\left|\frac{2L_x}{r^3}\right|0\right\rangle}{(E_n-E_0)} + \frac{\left\langle 0\left|\frac{2L_x}{r^3}\right|n\right\rangle\left\langle n|L_x|0\right\rangle}{(E_n-E_0)} \right\} \quad (2)$$

$$\delta_{22} = \frac{e^2}{2m}\left\langle 0\left|\frac{x^2+z^2}{r^3}\right|0\right\rangle - \left(\frac{e\hbar}{2m}\right)^2 \times \sum_n \left\{ \frac{\left\langle 0|L_y|n\right\rangle\left\langle n\left|\frac{2L_y}{r^3}\right|0\right\rangle}{(E_n-E_0)} + \frac{\left\langle 0\left|\frac{2L_y}{r^3}\right|n\right\rangle\left\langle n|L_y|0\right\rangle}{(E_n-E_0)} \right\} \quad (3)$$

where $L = L_x\hat{i} + L_y\hat{j} + L_z\hat{k}$ is the angular momentum. The first part of the above three equations regarding principal components of CSA tensor is generated by electrons resides in the spherically symmetric 's' orbital. The second term arise when the electrons are in 'p' or 'd' orbital. The isotropic component of chemical shift $\left(\delta_{iso} = \frac{\delta_{11}+\delta_{22}+\delta_{33}}{3}\right)$ represents the average values of the principal components of CSA tensor along three orthogonal directions. Basically, it is the position of the centre of gravity of the spinning CSA sideband pattern.[42,45,46] The breadth of the CSA tensor is getting affected due to the change of the centre of gravity of the spinning CSA pattern. Small changes in centre of gravity of CSA pattern is generally associated with larger change in chemical shift anisotropy.[47] According to Haeberlen convention[54] the asymmetry parameter is $\eta = \frac{\delta_{22}-\delta_{11}}{\delta_{33}-\delta_{iso}}$. The deviation of the spinning CSA side band pattern from its axially symmetric shape is measured by the asymmetry parameter. The sign of the asymmetry parameter indicates the direction of largest separation with respect to the centre of gravity of CSA pattern. 'Skew' $\left(k = \frac{3(\delta_{22}-\delta_{iso})}{\Omega}\right)$ says the amount of orientation of the asymmetry pattern. The width of the sideband pattern is called 'span' ($\Omega = \delta_{11} - \delta_{33}$).

The spinning CSA sideband pattern becomes axially symmetric, when δ_{22} is equal to δ_{11} or δ_{33}. Table 2 says that the asymmetry parameter is zero for C11, C17, C26, it is very small (≤0.3) for C2, C5, C10, C22, C23, C24, and very large (≥0.9) for C3, C4, C6, C18, C19, C21. When it is zero, the CSA pattern is called axially symmetric. On the contrary, the CSA pattern is highly asymmetric, when the asymmetry parameter is very large.

Fig. 3 shows ^{13}C 2DPASS CP MAS NMR spectrum of clocortolone pivalate. The direct-dimension and indirect-dimension of two-dimensional spectrum respectively represents the isotropic spectrum and anisotropic spectrum. The spinning CSA sideband patterns of (a) C14, (b) C22, (c) C26, (d) C13, (e) C6, (f) C4, (g) C20, (h) C18, (i) C9 carbon nuclei are also shown in Fig. 3. The different values of CSA parameters at

Table 2 The CSA parameters at structurally and chemically distinct carbon sites of clocortolone pivalate

Carbon from different chemical environment with isotropic chemical shift (δ_{iso}) (ppm)	δ_{11}	δ_{22}	δ_{33}	Span (ppm)	Skew	Anisotropy $\Delta\delta = \delta_{33} - \frac{(\delta_{11} + \delta_{22})}{2}$	Asymmetry $\eta = \frac{\delta_{22} - \delta_{11}}{\delta_{33} - \delta_{iso}}$
67.5(C1)	87.9	72	42.6	45.3	0.3	−37.3	0.6
52.3(C2)	82.7	41.8	32.3	50.4	−0.6	45.6	0.3
42.9(C3)	54.5	43.3	30.9	23.5	0.05	−17.9	0.9
88(C4)	113	87.1	64	49	−0.06	37.5	0.9
75.7(C5)	106.7	65.3	55.2	51.5	−0.6	46.4	0.3
34.7(C6)	46.6	34.5	22.9	23.7	−0.03	17.9	1
49(C7)	71.6	46.7	28.8	42.8	−0.2	33.9	0.8
36.1(C8)	46.3	38.1	24.1	22.2	0.3	−18.1	0.7
86.8(C9)	124.1	75.6	60.8	63.4	−0.5	55.9	0.4
70.1(C10)	109.7	55.2	45.5	64.2	−0.7	59.4	0.2
39.95(C11)	54.1	32.9	22.8	21.3	−1.0	21.2	0
17.7(C12)	29.8	15.1	8.2	21.6	−0.4	18.2	0.6
87.7(C13)	117.3	84	61.9	55.5	−0.2	44.4	0.7
165.7(C14)	287.9	149.1	59.9	228.1	−0.2	183.4	0.7
201.1(C15)	309.7	171.5	122.2	187.5	−0.5	162.9	0.5
20.6(C16)	36.4	16.8	8.7	27.7	−0.4	23.6	0.5
28.2(C17)	33.2	33.2	18.3	14.9	1	−14.9	0
156.6(C18)	269.8	150.6	49.3	220.5	−0.08	169.9	0.9
122(C19)	203.2	117.8	45	158.2	−0.08	121.8	0.9
84.8(C20)	118.7	78.3	57.3	61.4	−0.3	50.9	0.6
128.7(C21)	209.5	133.9	42.8	166.8	0.1	−129	0.9
187.9(C22)	300.1	151.2	112.6	187.5	−0.6	168.2	0.3
178.6(C23)	240.4	211	84.3	156.1	0.6	−141.4	0.3
46.4(C24)	59.2	53.2	26.8	32.5	0.6	−29.4	0.3
32.3(C25)	49.3	38.1	9.6	39.8	0.4	−34.1	0.5
23.5(C26)	42.5	14.1	14.1	28.4	−1	28.4	0
33.2(C27)	51.1	36.7	11.9	39.2	0.3	−32	0.7

numerous carbon sites of clocortolone pivalate indicate that the distribution of electron density surrounding the carbon nuclei, and the molecular conformation and orientation are dissimilar at different portion of the molecule. Fig. 4(b) and Table 2 show anisotropy parameter (defined as $\Delta\delta = \delta_{33} - \frac{(\delta_{11} + \delta_{22})}{2}$ according to Haeberlen convention[54]) is significantly high for C14, C15, C18, C19, C21, C22, and C23 nuclei, connected with neighbouring atoms by double bond. For carbonyl group carbon like C15, C22, C23 does not possess any axis of symmetry. The polarization is induced on the non spherical distribution of charges surrounding the carbon nuclei due to the electrostatic interaction. The strength of the induced magnetic field is getting influenced by the action of the polarization. Consequently, the induced magnetic field is varied along different directions. This is equally considered as reason behind the large value of anisotropy of carbonyl group carbon.[55] Another reason is magnetic anisotropy, which arise due to three miscellaneous values of magnetic susceptibilities $(\mathcal{X}_x, \mathcal{X}_y, \mathcal{X}_z)$ along three directions in principal axes system (PAS). Consequently, there originate an anisotropic susceptibility parallel to the magnetic field $(\Delta\mathcal{X}_{\parallel} = \mathcal{X}_z - \mathcal{X}_x)$ and perpendicular to the magnetic field $(\Delta\mathcal{X}_{\perp} = \mathcal{X}_y - \mathcal{X}_x)$.[55] The McConnell equation of magnetic anisotropy for carbonyl group is[56]

$$\delta_{anis} = \{\Delta\mathcal{X}_{\parallel}(3\cos^2\theta_1 - 1) + \Delta\mathcal{X}_{\perp}(3\cos^2\theta_2 - 1)\}/3R^3 \quad (4)$$

where θ_1 is the angle between the radius vector and x-axis. θ_2 is the angle between the radius vector and z-axis. Effective magnetic field experienced by the nucleus varies along three orthogonal directions because of these anisotropic magnetic susceptibilities.

The existence of the non-bonded electron surrounding the nucleus is responsible for the manifestation of magnetic shielding and deshielding effect.[57] When the non-bonded electron revolves around the nucleus in a clockwise direction, a paramagnetic current is generated, and a magnetic field is induced along the direction of the external magnetic field. Naturally, the strength of the local magnetic field is increased. This effect is called magnetic deshielding effect. On the other hand, when a bonded electron revolves around the nucleus along the counter clockwise direction, a magnetic field is generated along the opposite direction of the external magnetic field. As a consequence, the value of the local magnetic field is decreased – magnetic shielding effect. These effects manifest themselves as a large value of chemical shift anisotropy for those carbon nuclei surrounded by nonspherical distribution of electronic charge density.

3.3 Determination of correlation times associated with molecular motions

The molecular motions associated with molecular rotation, translational self-diffusion, and internal motion in non-rigid

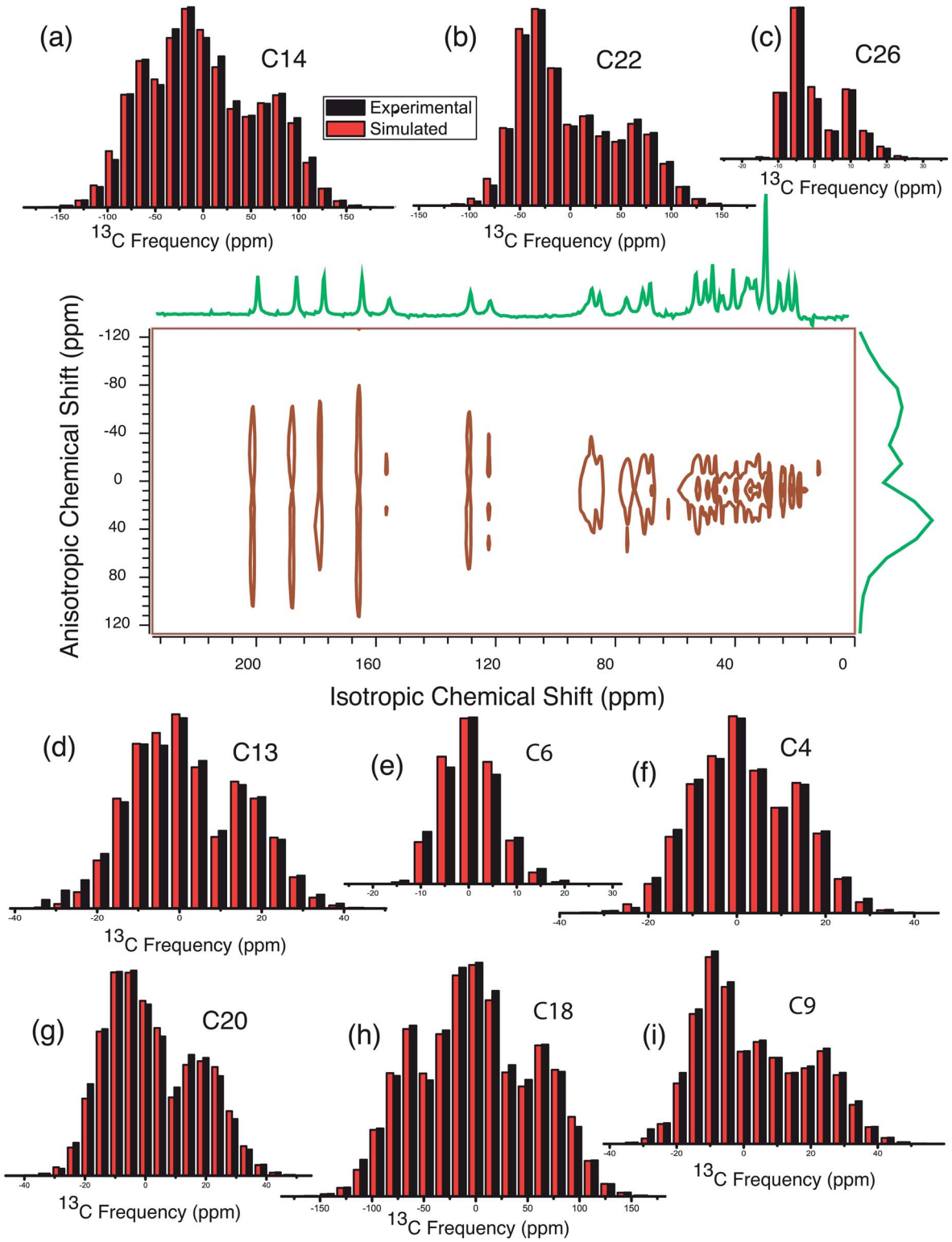

Fig. 3 ^{13}C 2DPASS CP MAS NMR spectrum of clocortolone pivalate. The horizontal axis shows isotropic spectrum, and the vertical axis shows anisotropic spectrum. The spinning CSA sideband patterns of (a) C14, (b) C22, (c) C26, (d) C13, (e) C6, (f) C4, (g) C20, (h) C18, (i) C9 are shown in this figure.

molecular can be probed by nuclear spin relaxation. Several nuclear interactions like chemical shift anisotropy interaction, magnetic dipole–dipole interaction, the spin rotation interaction, the electric quadrupole interaction, and the scalar coupling of the first and second kind simultaneously contribute to the relaxation mechanism of a spin system. However, for ^{13}C

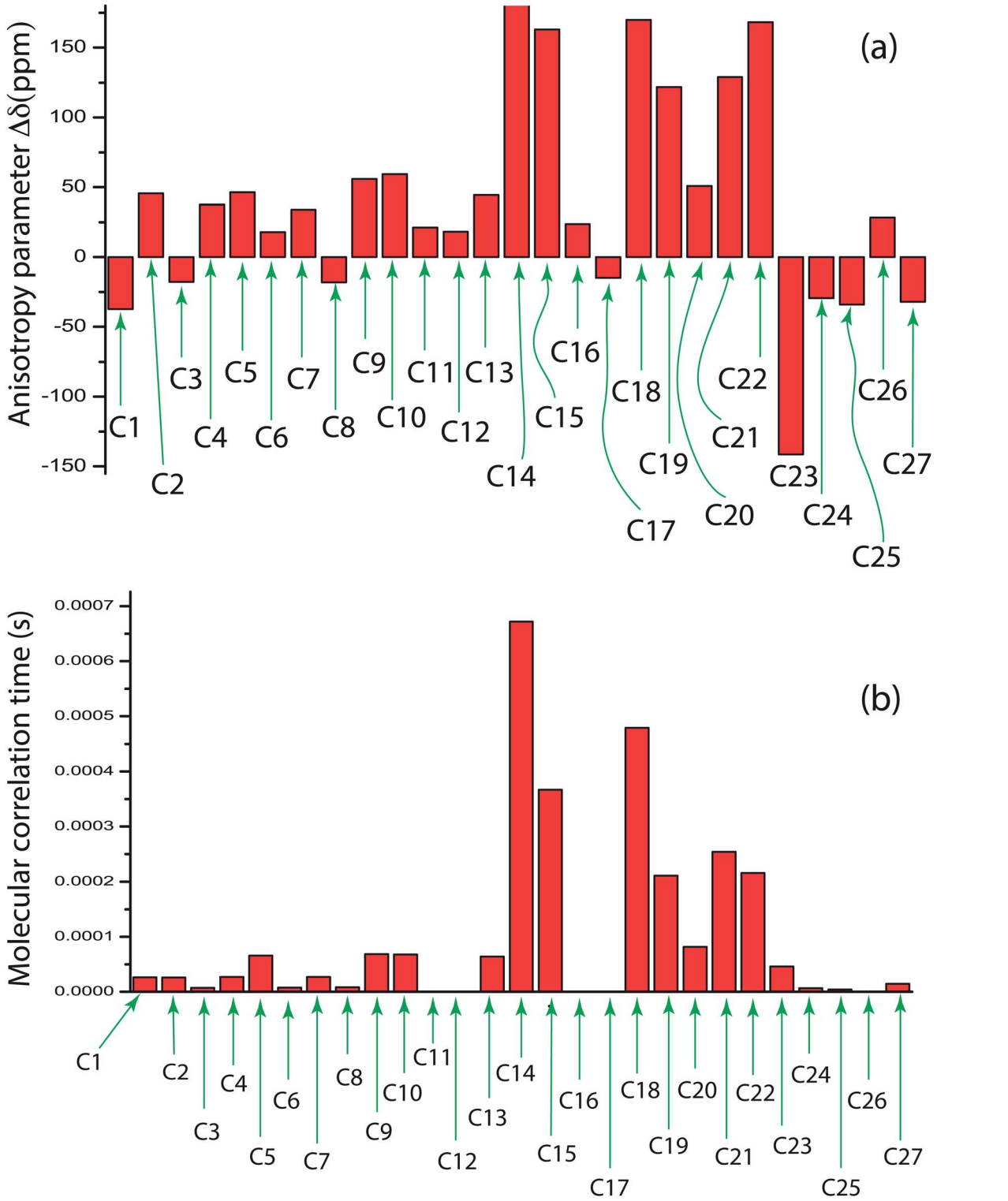

Fig. 4 (a) Bar-diagram of anisotropy parameter at chemically different carbon sites of clocortolone pivalate. (b) Bar-diagram of molecular correlation time at chemically different carbon sites. Molecular correlation time is high for those nuclei for which the value of chemical shift anisotropy parameter ($\Delta\delta$) is high and *vice versa*.

nuclei, the relaxation mechanism is predominated by the chemical shift anisotropy interaction, and the hetero-nuclear dipole–dipole coupling. The magnitude of CSA tensor fluctuates with time because of the modulations caused by molecular rotations. The chemical shift anisotropy has a great influence in relaxation mechanism for nuclei exhibiting large chemical-shift ranges. The expression of spin–lattice relaxation time due to CSA interaction is[46,48,49,53]

$$\frac{1}{T_1^{CSA}} = \frac{2}{15}\gamma^2 B^2 S^2 \left(\frac{\tau_2}{1 + \omega^2\tau_2^2}\right) \quad (5)$$

The correlation time $\tau_c = 3\tau_2$ and B is the applied external field. Where $S^2 = (\Delta\delta)^2(1 + \eta^2/3)$ and $\left[\Delta\delta = \delta_{33} - \frac{(\delta_{22} + \delta_{11})}{2}\right]$, $\left(\eta = \frac{\delta_{22} - \delta_{11}}{\delta_{33} - \delta_{iso}}\right)$.

The contribution of dipole–dipole interaction on spin–lattice relaxation is[48,53]

$$\frac{1}{T_1^{DD}} = \frac{1}{10}\left(\frac{\gamma_C\gamma_X\hbar}{r_{CX}^3}\right)^2 \tau_2 \left[\frac{3}{1 + \omega_C^2\tau_2^2} + \frac{1}{1 + (\omega_X - \omega_C)^2\tau_2^2} + \frac{6}{1 + (\omega_X - \omega_C)^2\tau_2^2}\right] \quad (6)$$

By keeping first term only of the above expression

$$\frac{1}{T_1^{DD}} = \frac{1}{10}\left(\frac{\gamma_C\gamma_X\hbar}{r_{CX}^3}\right)^2 \tau_2 \left[\frac{3}{1 + \omega_C^2\tau_2^2}\right] \quad (7)$$

where X represent ^{1}H, ^{35}Cl, and ^{19}F. The bond distance r_{CX} is represented in Table 4. Larmor precession frequency $\omega = 2\pi f = 2 \times 3.14 \times 125.758$ MHz $= 789.76024$ MHz; $B = 11.74$ T, $\gamma_C = 10.7084$ MHz T^{-1}, $\gamma_H = 42.577$ MHz T^{-1}, $\gamma_N = 3.077$ MHz T^{-1}. $\hbar = 1.054 \times 10^{-34}$ J s.

The spin–lattice relaxation for ^{13}C can be written as

$$\frac{1}{T_1} = \frac{1}{T_1^{CSA}} + \frac{1}{T_1^{DD}} = \frac{2}{15}\gamma^2 B^2 S^2 \left(\frac{\tau_2}{1 + \omega^2\tau_2^2}\right) + \frac{1}{10}\left(\frac{\gamma_C\gamma_X\hbar}{r_{CX}^3}\right)^2 \tau_2 \left[\frac{3}{1 + \omega_C^2\tau_2^2}\right] \quad (8)$$

At the presence of high magnetic field, chemical shift anisotropy (CSA) interaction dominate over hetero-nuclei dipole–dipole coupling for non-protonated carbon nuclei.[48,49] Molecular correlation time is calculated by eqn (8).

Table 3 and Fig. 4(b) show molecular correlation time, which implies the time required for the rotation of the molecule through one radian, of clocortolone pivalate at chemically different carbon sites. The order of magnitude varies from 10^{-4} to 10^{-8} s. Molecular correlation time is of the order of 10^{-4} s for those carbon nuclei attached with neighbouring carbon or oxygen atoms by double bonds like C14, C15, C18, C19, C21, C22, and C23(as shown in Fig. 1(a)). It implies the molecular correlation time is substantially high for those carbon nuclei associated with high values of chemical shift anisotropy parameter ($\Delta\delta$). On the contrary, molecular correlation time is of the order of 10^{-8} s for C12, C16, C17 carbon nuclei reside at the side portion of the molecule and the magnitude of chemical shift anisotropy parameter ($\Delta\delta$) is low for those carbon nuclei. Fig. 4 shows the bar diagram of chemical shift anisotropy parameter ($\Delta\delta$) and molecular correlation time at crystallographically and chemically different carbon nuclei sites.

The crystal structure of the molecule was first drawn by using Chem Draw software.[24,58] The structure was optimized by density functional theory method with the help of GAUSSIAN 09W software.[59] B3LYP-631G (d, p) basis set was used for the optimization process. The bond distances, shown in Table 4, were extracted from the final optimized structure of clocortolone pivalate.

The considerable variation of the spin–lattice relaxation time (Table 1), CSA parameters (Table 2) and molecular correlation time (Table 3) at numerous carbon nuclei sites of clocortolone pivalate, suggests that the nuclear spin dynamics hugely varied due to the presence of the different structural groups surrounding the carbon nuclei. How the dynamics of carbon nuclei spin of clocortolone pivalate is getting affected due to the presence of various chemical group surrounding the nuclei can be picturized vividly by this type of extensive studies. The drug, clocortolone pivalate has different substitution pattern for example methylation at C8, chlorine at C4 and fluorine at C13 and pivalate at C20 *etc.* These unique substitution patterns make it different from other steroids to be more potent, safe, efficacious and metabolically stable. Thus, dynamics at every chemically different carbon nuclei is important in this aspect.

Table 3 Molecular correlation time at chemically different carbon sites of clocortolone pivalate

Carbon nuclei	Molecular correlation time (s)	Carbon nuclei	Molecular correlation time (s)
C1	2.6×10^{-5}	C2	2.6×10^{-5}
C3	7.4×10^{-6}	C4	2.7×10^{-5}
C5	6.6×10^{-5}	C6	7.7×10^{-6}
C7	2.7×10^{-5}	C8	8.3×10^{-6}
C9	6.9×10^{-5}	C10	6.8×10^{-5}
C11	2.9×10^{-7}	C12	5.9×10^{-8}
C13	6.4×10^{-5}	C14	6.7×10^{-4}
C15	3.7×10^{-4}	C16	9.7×10^{-8}
C17	3.5×10^{-8}	C18	4.8×10^{-4}
C19	2.1×10^{-4}	C20	8.2×10^{-5}
C21	2.5×10^{-4}	C22	2.2×10^{-4}
C23	4.6×10^{-5}	C24	6.6×10^{-6}
C25	4.2×10^{-6}	C26	1.3×10^{-7}
C27	1.5×10^{-5}		

Table 4 Bond-distances of clocortolone pivalate

Bond-distance of clocortolone pivalate			
Bond	Distance (Å)	Bond	Distance (Å)
C1–H1	1.088	C15–H15	1.092
C1–C2	1.337	C15–H16	1.096
C1–C10	1.524	C15–H17	1.095
C2–H2	1.084	C16–H18	1.100
C2–C3	1.475	C16–C17	1.527
C3–O1	1.227	C17–H19	1.095
C3–C4	1.478	C17–H20	1.096
C4–H3	1.085	C17–C18	1.551
C4–C5	1.343	C18–C20	1.555
C5–C6	1.510	C18–H21	1.097
C5–C10	1.539	C18–C19	1.526
C6–H4	1.095	C19–H22	1.095
C6–F	1.366	C19–H23	1.095
C6–C7	1.525	C19–H24	1.095
C7–H5	1.097	C20–C21	1.495
C7–H6	1.097	C20–H25	1.099
C7–C8	1.539	C21–C22	1.514
C8–C9	1.582	C21–O3	1.230
C8–C16	1.537	C22–H26	1.095
C8–H7	1.095	C22–C27	1.092
C9–Cl	1.865	C22–O4	1.412
C9–C10	1.598	O4–C23	1.375
C9–C12	1.572	C23–O5	1.225
C10–C11	1.505	C23–C24	1.532
C11–H8	1.093	C24–C25	1.535
C11–H9	1.099	C24–C26	1.535
C11–H10	1.095	C24–C27	1.535
C12–C13	1.505	C25–H28	1.096
C12–O2	1.424	C25–H29	1.096
C12–H11	1.097	C25–H30	1.096
O2–H12	0.972	C26–H31	1.096
C13–H13	1.096	C26–H32	1.096
C13–H14	1.097	C26–H33	1.096
C13–C14	1.541	C27–H34	1.096
C14–C15	1.551	C27–H35	1.096
C14–C16	1.543	C27–H36	1.096
C14–C20	1.550		

4. Conclusion

The correlation between the structure and dynamics of clocortolone pivalate (extensively used for cutaneous disease states, such as psoriasis vulgaris, nummular eczema, contact dermatitis, atopic dermatitis, seborrheic dermatitis, and stasis dermatitis) are monitored by measuring CSA parameters, spin–lattice relaxation time, and molecular correlation time at twenty-seven crystallographically and chemically different carbon nuclei sites. The CSA parameters are substantially varied at chemically different carbon sites, indicate that the molecular orientation and electron distribution are different in numerous regions of this molecule. The asymmetry parameter is zero for C11, C17, C26, indicates that the spinning CSA sideband pattern for those nuclei are axially symmetric. And it is very small ($\leq$0.3) for C2, C5, C10, C22, C23, C24, resonance line, suggests the spinning CSA side-band pattern for those resonance lines is nearly axially symmetric. On other hand, the spinning CSA sideband pattern is highly asymmetric for C3, C4, C6, C18, C19, C21 carbon resonance line. Anisotropy parameter is substantially high for double bonded C14, C15, C18, C19, C21, C22, and C23 nuclei. Spin–lattice relaxation time and molecular correlation time at chemically different carbon site of this molecule differ widely. Spin–lattice relaxation rate is slow for carbon nuclei reside at the carbon ring. On the contrary, it is very fast for C12, C17, C16, C26 carbon nuclei reside at the side portion of the molecule. Molecular correlation time is of the order of 10^{-4} s for those carbon nuclei attached with neighbouring carbon or oxygen atoms by double bonds like C14, C15, C18, C19, C21, C22, and C23. It implies that the molecular correlation time is very high for those carbon nuclei associated with high values of chemical shift anisotropy. On the contrary, molecular correlation time is of the order of 10^{-8} s for C12, C16, and C17 carbon nuclei present at the side portion of the molecule. The various portion of the molecule exhibit different degree of motions. The relationship between the structure and dynamics of the molecule is pictured by these types of investigation. This type of inclusive investigation will deliver a potential impact on the way of inventing advanced medicine in pharmaceutical industry.

Conflicts of interest

There are no conflicts to declare.

Acknowledgements

The author Manasi Ghosh is greatful to Science and Engineering Research Board (SERB), Department of Science and Technology (DST), Government of India (file no. EMR/2016/000249), and UGC-BSR (file no. 30-12/2014 (BSR)) for financial support.

References

1 J. M. Hanifin, K. D. Cooper, V. C. Ho, S. Kang, B. R. Krafchik, D. J. Margolis, L. A. Schachner, R. Sidbury, S. E. Whitmore, C. K. Sieck and A. S. Van Voorhees, Guidelines of care for atopic dermatitis, *J. Am. Acad. Dermatol.*, 2004, **50**, 391–404.
2 D. Y. Leung, R. A. Nicklas, J. T. Li, I. L. Bernstein, J. Blessing-Moore, M. Boguniewicz, J. A. Chapman, D. A. Khan, D. Lang, R. E. Lee and J. M. Portnoy, Disease management of atopic dermatitis: an updated practice parameter, *Ann. Allergy, Asthma, Immunol.*, 2004, **93**, S1–S21.
3 H. Saeki, M. Furue, F. Furukawa, M. Hide, M. Ohtsuki, I. Katayama, R. Sasaki, H. Suto and K. Takehara, Guidelines for management of atopic dermatitis, *J. Dermatol.*, 2009, **36**, 563–577.
4 J. Bourke, I. Coulson and J. English, Guidelines for the management of contact dermatitis: an update, *Br. J. Dermatol.*, 2009, **160**, 946–954.
5 A. Menter, N. J. Korman, C. A. Elmets, S. R. Feldman, J. M. Gelfand, K. B. Gordon, A. Gottlieb, J. Y. Koo, M. Lebwohl, H. W. Lim and A. S. Voorhees, Guidelines of care for the management of psoriasis and psoriatic

arthritis: section 3. Guidelines of care for the management and treatment of psoriasis with topical therapies, *J. Am. Acad. Dermatol.*, 2009, **60**, 643–659.

6 B. Brazzini and N. Pimpinelli, New and established corticosteroids in dermatology, *Am. J. Clin. Dermatol.*, 2002, **3**, 47–58.

7 I. C. Valencia and F. A. Kerdel, *Topical corticosteroids. Fitzpatrick's dermatology in general medicine*, ed. Wolff K., Goldsmith L. A., Katz S. I., Gilchrest B. A., Paller A. S. and Leffell D. J., McGraw-Hill, New York, 7th edn, 2008, pp. 2102–2106.

8 K. L. Goa, Clinical pharmacology and pharmacokinetic properties of topically applied corticosteroids: a review, *Drugs*, 1988, **36**, 51–61.

9 S. E. Jacob and T. Steele, Corticosteroid classes: a quick reference guide including patch test substances and cross-reactivity, *J. Am. Acad. Dermatol.*, 2006, **54**, 723–727.

10 M. W. Greaves, *Pruritus. Rook's textbook of dermatology*, T. Burns, S. Breathnach, N. Cox and C. Griffiths, Wiley-Blackwell, 8th edn, 2010, pp. 21.1–21.18.

11 B. M. Magnusson, S. E. Cross, G. Winckle and M. S. Roberts, Percutaneous absorption of steroids: determination of *in vitro* permeability and tissue reservoir characteristics in human skin layers, *Skin Pharmacol. Physiol.*, 2006, **19**, 336–342.

12 J. Bikowski, R. Pillai and B. Shroot, The position not the presence of the halogen in corticosteroids influences potency and side effects, *J Drugs Dermatol.*, 2006, **5**, 125–130.

13 M. Katz and E. H. Gans, Topical corticosteroids, structure–activity and the glucocorticoid receptor: discovery and development process of "planned serendipity", *J. Pharm. Sci.*, 2008, **97**, 2936–2947.

14 P. Buchwald, Glucocorticoid receptor binding: a biphasic dependence on molecular size as revealed by the bilinear LinBiExp model, *Steroids*, 2008, **73**, 193–208.

15 C. Holden, J. English, C. Hoare, A. Jordan, S. Kownacki, R. Turnbull and R. C. Staughton, Advised best practice forthe use of emollients in eczema and other dry skin conditions, *J. Dermatol. Treat.*, 2002, **13**, 103–106.

16 M. R. Warner and C. Camsia, *Topological corticosteroids. Comprehensive Dermatologic Drug therapy*, Saunders, Philadelphia, 2nd edn, 2007, pp. 595–624.

17 J. Q. Del Rosso and L. H. Kircik, A comprehensive review of clocortolone pivalate 0.1% cream: structural development, formulation characteristics, and studies supporting treatment of corticosteroid-responsive dermatoses, *The Journal of Clinical and Aesthetic Dermatology*, 2012, **5**, 20–24.

18 L. H. Kricik and J. Q. Del Rosso, The treatment of inflammatory facial dermatoses with cortical corticosteroids: focus on clocortolone pivalate 0.1% cream, *J Drugs Dermatol.*, 2012, **5**, 1194–1198.

19 J. Q. Del Rosso and L. H. Kircik, Transitioning from brand to generic with topical products and the importance of maintaining the formulation and therapeutic profiles of the original product : focus on clocortolone pivalate 0.1% cream, *J Drugs Dermatol.*, 2014, **13**, s77–s83.

20 L. H. Kircik, A study to assess the occlusivity and moisturization potential of three topical corticosteroid productus using the skin trauma after razor shaving (STARS) bioassay, *J Drugs Dermatol.*, 2014, **13**, 582–585.

21 J. Q. Del Rosso and L. H. Kircik, The role of a midpotency topical corticosteroid and the clinical relevance of formulation characteristics in the management of commonly encountered eczematous and inflammatory dermatoses in adults and children: focus on the pharmacologic properties of clocortolone pivalate 01% cream, *J Drugs Dermatol.*, 2013, **12**, s5–s10.

22 L. H. Kircik, Clocortolone pivalate: a topical corticosteroid with a unique structure, *J Drugs Dermatol.*, 2013, **12**, s3–s4.

23 S. Singh and B. K. Mann, Clinical utility of clocortolone pivalate for the treatment of corticosteroid-responsive skin disorders: a systematic review, *Clin. Cosmet. Investig. Dermatol.*, 2012, **5**, 61–68.

24 W. Xu, X. Jia, W. Liu, X. Zhang, Y. Chen, L. Zhou and S. You, Identification and characterization of three impurities in clocortolone pivalate, *J. Pharm. Biomed. Anal.*, 2012, **62**, 167–171.

25 D. A. Torchia, The measurement of proton-enhanced carbon-13 T1 values by method which suppresses artifacts, *J. Magn. Reson.*, 1978, **30**, 613.

26 R. Tycko, G. Dabbagh and P. A. Mirau, Determination of chemical shift anisotropy lineshapes in a two-dimensional magic angle spinning NMR experiment, *J. Magn. Reson.*, 1989, **85**, 265–274.

27 S. F. Liu, J. D. Mao and K. Schmidt-Rohr, A robust technique for two-dimensional separation of undistorted chemical shift anisotropy powder patterns in magic angle spinning NMR, *J. Magn. Reson.*, 2002, **155**, 15–28.

28 J. C. C. Chan and R. Tycko, Recoupling of chemical shift anisotropies in solid state NMR under high speed magic angle spinning and in uniformly ^{13}C labelled systems, *J. Chem. Phys.*, 2003, **118**, 8378–8389.

29 G. Hou, L. Byeon In-Ja, J. Ahn, A. M. Gronenborn and T. Polenova, Recoupling of chemical shift anisotropy by R-symmetry sequences in magic angle spinning NMR spectroscopy, *J. Chem. Phys.*, 2012, **137**, 134201–134210.

30 A. Bax, N. M. Szeverenyi and G. E. Maciel, Correlation of isotropic shifts and chemical shift anisotropies by two-dimensional Fourier-transform magic angle hopping NMR spectroscopy, *J. Magn. Reson.*, 1983, **52**, 147–152.

31 A. Bax, N. M. Szeverenyi and G. E. Maciel, Chemical shift anisotropy in powdered solids studied by 2D FT CP/MAS NMR, *J. Magn. Reson.*, 1983, **51**, 400–408.

32 A. Bax, N. M. Szeverenyi and G. E. Maciel, Chemical shift anisotropy in powdered solids studied by 2D FT NMR with flipping of the spinning axis, *J. Magn. Reson.*, 1983, **55**, 494–497.

33 Z. Gan, High-resolution chemical shift and chemical shift anisotropy correlation in solids using slow magic angle spinning, *J. Am. Chem. Soc.*, 1992, **114**, 8307–8309.

34 W. T. Dixon, Spinning-sideband-free and spinning-sideband-only NMR spectra in spinning samples, *J. Chem. Phys.*, 1982, **77**, 1800–1809.

35 O. N. Antzutkin, S. C. Shekar and M. H. Levitt, Two-dimensional sideband separation in magic angle spinning NMR, *J. Magn. Reson., Ser. A*, 1995, **115**, 7–19.

36 B. J. Walder, K. K. Dey, D. C. Kaseman, J. H. Baltisberger and P. J. Grandinetti, Sideband separation experiments in NMR with phase incremented echo train acquisition, *J. Chem. Phys.*, 2013, **138**, 174203.

37 M. Ghosh, S. Sadhukhan and K. K. Dey, Elucidating the internal structure and dynamics of α-chitin by 2DPASS-MAS-NMR and spin–lattice relaxation measurements, *Solid State Nucl. Magn. Reson.*, 2019, **97**, 7–16.

38 M. Ghosh, B. P. Prajapati, N. Kango and K. K. Dey, A comprehensive and comparative study of the internal structure and dynamics of natural β-keratin and regenerated β-keratin by solid state NMR spectroscopy, *Solid State Nucl. Magn. Reson.*, 2019, **101**, 1–11.

39 M. Ghosh, N. Kango and K. K. Dey, Investigation of the internal structure and dynamics of cellulose by ^{13}C-NMR relaxometry and 2DPASS-MAS-NMR measurements, *J. Biomol. NMR*, 2019, **73**, 601–616.

40 K. K. Dey and M. Ghosh, Understanding the effect of deacetylation on chitin by measuring chemical shift anisotropy tensor and spin lattice relaxation time, *Chem. Phys. Lett.*, 2020, **738**, 136782.

41 K. K. Dey, S. Gayen and M. Ghosh, Investigation of the detailed internal structure and dynamics of itraconazole by solid state NMR measurements, *ACS Omega*, 2019, **4**, 21627–21635.

42 J. Herzfeld and A. E. Berger, Sideband intensities in NMR spectra of samples spinning at the magic angle, *J. Chem. Phys.*, 1980, **73**, 6021–6030.

43 N. F. Ramsey, Magnetic Shielding of Nuclei in Molecules, *Phys. Rev.*, 1950, **78**, 699–703.

44 N. F. Ramsey, Chemical effects in nuclear magnetic resonance and in diamagnetic susceptibility, *Phys. Rev.*, 1952, **86**, 243–246.

45 A. M. Orendt and J. C. Facelli, Solid state effects on NMR chemical shifts, *Annu. Rep. NMR Spectrosc.*, 2007, **62**, 115–178.

46 M. P. Nicholas, E. Eryilmaz, F. Ferrage, D. Cowburn and R. Ghose, Nuclear spin relaxation in isotropic and anisotropic media, *Prog. Nucl. Magn. Reson. Spectrosc.*, 2010, **57**, 111–158.

47 N. Tjandra, A. Szabo and A. Bax, Protein backbone dynamics and 15B chemical shift anisotropy from quantitative measurement of relaxation interference effects, *J. Am. Chem. Soc.*, 1996, **118**(29), 6986–6991.

48 P. Dais and A. Spyros, ^{13}C nuclear magnetic relaxation and local dynamics of synthetic polymers in dilute solution and in the bulk state, *Prog. Nucl. Magn. Reson. Spectrosc.*, 1995, **27**, 555–633.

49 F. A. L. Anet and D. J. O'Leary, The shielding tensor part II: understanding its strange effect on relaxation, *Concepts Magn. Reson.*, 1992, **4**, 35–52.

50 D. Massiot, V. Montauillout, F. Fayon, P. Florian and C. Bessada, Order-resolved sideband separation in magic angle spinning NMR of half integer quadrupolar nuclei, *Chem. Phys. Lett.*, 1997, **272**, 295–300.

51 F. Fayon, C. Bessada, A. Douy and D. Massiot, Chemical bonding of lead in glasses through isotropic *vs.* anisotropic correlation: PASS shifted Echo, *J. Magn. Reson.*, 1999, **137**, 116–121.

52 M. S. Ironside, R. S. Stein and M. J. Duer, Using chemical shift anisotropy to resolve isotropic signals in solid-state NMR, *J. Magn. Reson.*, 2007, **188**, 49–55.

53 R. Y. Dong, NMR relaxation rates, *Encyclopedia of Spectroscopy and Spectrometry*, 1999, pp. 1568–1575, DOI: 10.1006/rwsp.2000.0264.

54 U. Haeberlen, *High Resolution NMR in Solids: Selective Averaging*, Academic Press, New York, 1976.

55 R. J. Abraham, M. Mobli and R. J. Smith, ^{1}H chemical shifts in NMR: Part 19† carbonyl anisotropies and steric effects in aromatic aldehydes and ketones, *Magn. Reson. Chem.*, 2003, **41**, 26–36.

56 H. M. McConnell, Theory of Nuclear Magnetic Shielding in Molecules: Long-Range Dipolar Shielding of protons, *J. Chem. Phys.*, 1957, **27**, 226.

57 M. Randic, M. Novic and D. Plavsic, π-Electron currents in fixed π-sextet aromatic benzenoids, *J. Math. Chem.*, 2012, **50**, 2755–2774.

58 L. D. Mendelsohn, ChemDraw 8 ultra, windows and macintosh versions, *J. Chem. Inf. Comput. Sci.*, 2004, **44**(6), 2225–2226.

59 M. J. Frisch, G. W. Trucks, H. B. Schlegel, G. E. Scuseria, M. Robb, J. R. Cheeseman, G. Scalmani, V. Barone, B. Mennucci, G. A. Petersson and H. Nakatsuji, *Gaussian 09, Revision D. 01*, Gaussian. Inc., Wallingford, CT, 2009.